Catalysis Science & Technology

Cyclohexene Epoxidation with H_2O_2 in the Vapor and Liquid Phases over a Vanadium-based Metal-Organic Framework

Journal:	*Catalysis Science & Technology*
Manuscript ID	CY-ART-04-2020-000833.R1
Article Type:	Paper
Date Submitted by the Author:	12-Jun-2020

Complete List of Authors:	Yoon, Tae-Ung; Yonsei University, Department of Chemical and Biomolecular Engineering Ahn, Sol; Northwestern University, Kim, Ah-Reum; Yonsei University Department of Chemical and Biomolecular Engineering Notestein, Justin; Northwestern University, Chemical and Biological Engineering Farha, Omar; Northwestern University, Department of Chemistry Bae, Youn-Sang; Yonsei University, Department of Chemical and Biomolecular Engineering

ARTICLE

Cyclohexene Epoxidation with H_2O_2 in the Vapor and Liquid Phases over a Vanadium-based Metal-Organic Framework

Received 00th January 20xx,
Accepted 00th January 20xx

DOI: 10.1039/x0xx00000x

Tae-Ung Yoon, ‡[a] Sol Ahn, ‡[b] Ah-Reum Kim,[a] Justin M. Notestein,*[b] Omar K. Farha,*[bc] and Youn-Sang Bae*[a]

A metal–organic framework, MIL-47(V) containing coordinatively saturated V^{+IV} sites linked together by terephthalic linkers, was prepared by a solvothermal method and evaluated as a catalyst in the epoxidation of cyclohexene. We have compared the catalytic activity in the condensed and gas phase oxidation of cyclohexene to discuss the effect of temperature and reaction phase in cyclohexene epoxidation over MIL-47(V). The catalysts were examined for the epoxidation of cyclohexene with H_2O_2 at 50, 65, 120, and 150℃. We observed significant differences in product selectivity between liquid-phase and gas-phase operations and confirmed that the active sites are tightly incorporated into the MOF as nodes channels and thus resistant to leaching.

Introduction

Metal–organic frameworks (MOFs) are a class of crystalline porous solids that are promising new materials for many applications, especially those MOFs with good chemical and thermal stability. [1, 2] The high, and often selective, sorption capacities of these materials make them candidate materials for various applications including but not limited to gas separation, storage, sensing, capture and catalysis. [1, 3-5] Separately, alkene epoxidation is a challenging and important class of chemical reactions. For example, propylene oxide is one of the highest produced organic chemicals, at 7.5 million tons per year. [6, 7] Catalytic liquid-phase epoxidation of cyclohexene is commercially important for the production of cyclohexene oxide, an essential intermediate in fine chemicals manufacture. [8-10] It is also a widely-used probe reaction. Although not generally practiced, gas-phase epoxidation would be highly desirable, as it would avoid common problems in condensed phase catalysis, such as large reactor volumes, leaching of the catalytic metal sites, or competition for the active site by coordinating solvents. Vapor phase operation also allows higher reaction temperatures, and thus higher reaction rates, without high-pressure operation. [11-13]

A V-containing MOF specifically MIL-47(V) has been studied in epoxidation catalysis, both experimentally and theoretically. [14, 18] However, the previous reports have been focused on liquid-phase epoxidation of cyclohexene at 50°C. To the best of our knowledge, there were no reports on gas-phase oxidation of cyclohexane in MOFs including MIL-47(V).

In this study, we have compared the catalytic activity of MIL-47(V) in the condensed and gas phase oxidation of cyclohexene. MIL-47(V) consists of corner-sharing vanadium (III) oxide octahedral chains connected by terephthalate linkers (Figure 1). Catalytic studies on cyclohexene oxidation in MOFs have been published by several groups. [14, 16-18] However, these studies have seen low reaction rates or problems with active site leaching, which motivates both the study of catalytic node MOFs like MIL-47(V), and the study of epoxidation in the gas phase. This research discusses the effect of temperature and reaction phase in cyclohexene epoxidation over this catalyst. Different mechanisms appear to dominate in the gas and condensed phases, which contributes to the different selectivities and rates that are observed.

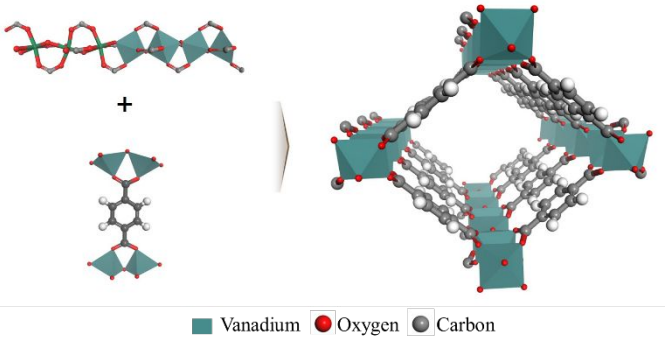

Figure 1. View of the MIL-47(V) structures. Left: chain of corner sharing $V^{4+}O_6$ octahedra and organic linker; Right: view along the chain axis, highlighting the 1D pores system.

[a] *Department of Chemical and Biomolecular Engineering, Yonsei University, 50 Yonsei-ro, Seodaemun-gu, Seoul 03722, Korea. E-mail: mowbae@yonsei.ac.kr.*
[b] *Department of Chemical and Biological Engineering, Northwestern University, 2145 Sheridan Road, Evanston, Illinois 60208, United States*
[c] *International Institute of Nanotechnology and Department of Chemistry, Northwestern University, 2145 Sheridan Road, Evanston, Illinois 60208, United States*

†Electronic Supplementary Information (ESI) available: Experimental details. See DOI: 10.1039/x0xx00000x

‡ These authors contributed equally.

Experimental Methods

Synthesis of Catalysts

The preparation of MIL-47(V) was carried out as previously reported. [19] Briefly, 1.224 g (0.0078 mmol) of vanadium (III) chloride (VCl_3; Sigma Aldrich, 97 %), 0.323 g (0.0019 mmol) of terephthalic acid (TPA, C_6H_4-1,4-$(CO_2H)_2$; Sigma Aldrich, 98 %) and 14.00 g (0.78 mmol) of deionized water were mixed in the molar ratio of 1 V : 0.25 TPA : 100 H_2O. The reactants were introduced to a Teflon-lined steel autoclave, sealed and placed in a convection oven at 200 ℃ for 4 days. After that, excess TPA was removed by dispersing the powder in excess N,N-dimethylformamide (DMF; Sigma Aldrich, 99 %) for 10 min with stirring. Then, filtration was performed to recover the powder. After that, the resulting powder was placed in a Teflon-lined steel autoclave with DMF. This autoclave was placed in an oven at 150 ℃ for overnight to further purify the powder with hot DMF. Finally, the MOF suspension was cooled and filtered, and the MOF samples were heated overnight at 250 ℃ under an air atmosphere to remove DMF.

Characterizations

Powder X-ray diffraction (PXRD) was performed using a STOE-STADI MP powder diffractometer (STOE, Germany) operating at 40 kV voltage and 40 mA current with Cu-Kα X-ray radiation (λ = 0.154056 nm) in transmission geometry. Diffraction patterns were collected on the $3° < 2\theta < 50°$ in 0.02° steps at 5°/min scan speed.

Brunauer-Emmett-Teller (BET) surface area was obtained from a N_2 adsorption isotherm at -196 ℃, which was measured using a Tristar II surface area and porosity analyzer (Micromeritics Instruments, USA). Before the N_2 adsorption experiment, the sample was activated at 150 ℃ for 15 h under vacuum. The BET surface area was calculated within the linear range determined by consistency criteria ($0.00079 < P/P_0 < 0.00512$). [20, 21] Total pore volume was estimated at $P/P_0 = 0.99$. Pore size distributions were determined by the DFT calculation method.

Inductively coupled plasma optical emission spectrometry (ICP-OES) was carried out using an iCAP 7600 (Thermo Scientific, USA). Vanadium (292.402, 309.311, 310.23, and 311.071 nm) contents were compared to the ICP standard solutions.

Diffuse reflectance infrared Fourier transform spectroscopy (DRIFTS) was performed using a Nicolet 6700 FTIR spectrometer (Thermo Scientific, USA) equipped with a liquid nitrogen cooled Mercury Cadmium Telluride (MCT) detector. The spectrum was collected in a KBr mixture and the pure KBr background was subtracted.

Liquid-phase Cyclohexene Epoxidation

Liquid-phase catalytic epoxidation was performed in 20 mL septum-cap glass vials vented with a needle. Cyclohexene (11 mmol, 1.1 mL, > 99 %, Sigma-Aldrich), and 1,2-dichlorobenzene as an internal standard (1.3 mmol, 150 µL, Sigma-Aldrich), were dissolved in acetonitrile (9 mL, Sigma-Aldrich), to which MIL-47(V) (6.7 mg, 29 µmol of vanadium) was added. After heating to 50 or 65 ℃ and shaking at 300 rpm for 1 h, the reaction was initiated with the addition of 4.0 M H_2O_2 in an acetonitrile solution (1.1 mmol, 270 µL). This H_2O_2 solution was prepared by diluting aqueous H_2O_2 (10 mL, 30 wt %, Sigma-Aldrich) in acetonitrile (20 mL), followed by drying over anhydrous $MgSO_4$ (7g, > 99 %, Sigma-Aldrich), which was then centrifuged and decanted. The initial molar ratio was cyclohexene : H_2O_2 : V = 400 : 40 : 1

Reaction aliquots were collected into gas chromatography (GC) sampling vials with silver powder (ca. 0.5 mg, > 99 %, Sigma-Aldrich) to quench unreacted H_2O_2. This prevents further oxidation of the reactant. Products from cyclohexene oxidation were identified and quantified using a Shimadzu 2010 GC-FID (Shimadzu, Japan) equipped with a TR-1 capillary column against calibrated standards. Carbon products observed in this reaction were cyclohexene oxide (epoxide), trans-1,2-cyclohexane diol (diol), 2-cyclohexen-1-one (cyclohexenone), and 2-cyclohexen-1-ol (cyclohexenol). For catalytic reactions, mass balances (products detected / reactant consumed) were ≥ 90 %.

A hot filtration was performed to test for catalyst leaching. Cyclohexene epoxidation was run for 15 min, then the reaction mixture was transferred using a syringe filter while the mixture remained stirring at 50 or 65 ℃. The transferred sample was placed in a clean, heated 20 mL septum-cap vial, where the reaction continued as usual.

Gas-phase Cyclohexene Epoxidation

The gas-phase epoxidation kinetic studies were carried out in a custom-built catalytic reaction system. [22] This system used a thermostatted quartz tube reactor, operated in a down-flow configuration. A fixed bed packed with a catalyst (47 mg, 0.078 mmol) was partially filled by a quartz wool plug. Hydrogen peroxide vapor was generated by feeding liquid H_2O_2 (same 4 M H_2O_2 solution as mentioned above) at 0.1 mL/h with a KDS 100 syringe pump (KD Scientific, USA) equipped with a plastic syringe through a FEP (fluorinated ethylene propylene) capillary tube to the top of the reactor, where the liquid evaporated at the temperature (110 °C) of the upper reactor furnace. Cyclohexene vapor was delivered using a 7.5 mL/min He flow (99.999%, Airgas) as a reactant through a quartz bubbler with additional dilution by a 20 mL/min He flow at 25 °C and nominal ambient pressure (vapor pressure: 11.9 kPa). The flowrates were adjusted with mass flow controllers (Brooks Instruments). Cyclohexene (4 kPa) and H_2O_2 (1.3 kPa) were fed at a ratio of 3:1. Reaction products were separated by a HP-INNOWAX column (50 m length, 0.2 mm diameter, 0.4 µm film) and were identified and quantitated with a flame ionization detector (FID) mounted on a 7890 A GC (Agilent Technologies). Carbon products observed in this reaction were diol, cyclohexenone, cyclohexenol, and cyclohexanone.

Results and discussion

Catalyst Characterizations

PXRD pattern of the as-synthesized sample matches well with the simulated pattern, [19] and the material maintains its crystallinity after liquid-phase and gas-phase reactions (Figure 2(a) and Figure S1). However, after gas-phase reaction, there is formation of a small amount of V_2O_5 as indicated by an asterisk (*). The BET surface area calculated from the nitrogen isotherm (1110 m^2/g, Figure 2(b)) agrees reasonably with the reported value (1050 m^2/g). [19, 23] In diffuse reflectance infrared Fourier transform spectra (DRIFTS), there was no big change after liquid-phase and gas-phase reactions (Figure2(c)).

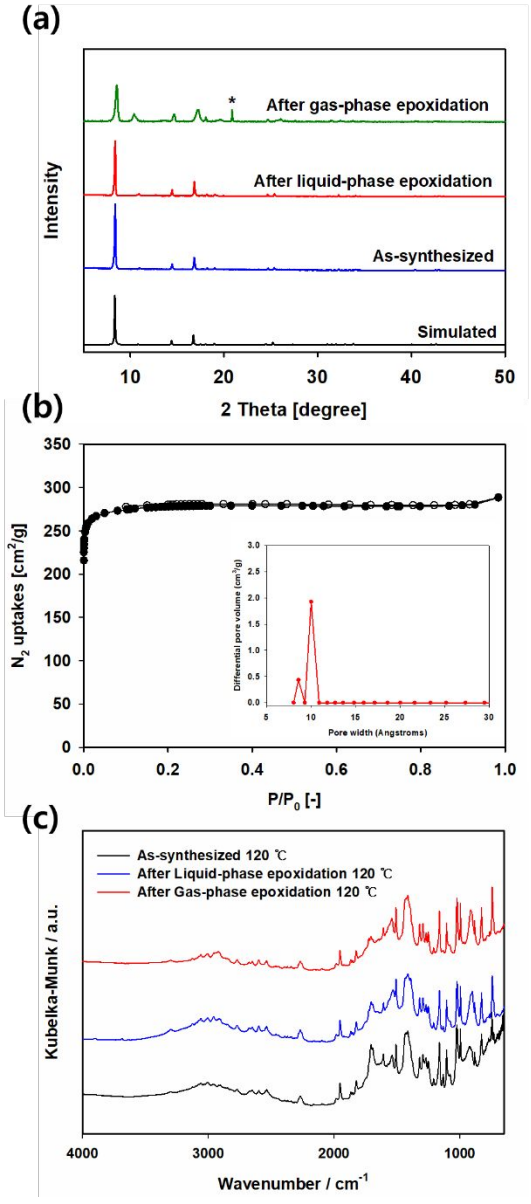

Figure 2. (a) X-ray powder diffraction patterns of MIL-47(V) after being degassed at 150 ℃, 15 h. (*: feature of V_2O_5) (b) N_2 adsorption-desorption isotherm at -196 ℃ on MIL-47(V) and pore size distribution calculated by density functional theory (DFT) method as an inset. (c) DRIFT spectra of as-synthesized MIL-47(V) and post reaction catalysts.

Liquid-phase epoxidation

Figures 3(a) and 3(c) present the detailed product distributions for MIL-47(V) catalyst as a function of reaction time at 65 ℃ and 50 ℃, respectively. Similar product distributions were obtained for reactions at both temperatures. The liquid-phase reaction products formed are epoxide, diol, cyclohexenone, and cyclohexenol. Scheme 1 illustrates the proposed reaction network for liquid-phase cyclohexene epoxidation, based on prior studies of cyclohexene epoxidation. [24-26]

The initial turnover frequency (up to 15 min or ~50% yield of C_6 oxygenates with respect to limiting H_2O_2) is 1.15 mol_{c6} mol_v^{-1} min^{-1}. Diol was observed initially at < 5 % selectivity. The low selectivity and the exclusive formation of the trans isomer is consistent with the diol being formed from the epoxide by hydrolysis. Figures 3(b) and 3(d) plot instantaneous selectivity against conversion. During this initial period, the production of cyclohexenol and cyclohexanone are high and similar. For this to be consistent with the reaction network in Scheme 1, most of the radical-derived hydroperoxyl species must be undergoing bimolecular decomposition (top route) and not contributing to further formation of epoxide via the middle route of Scheme 1. The ~ 25% selectivity to epoxide must therefore be formed via the direct activation of H_2O_2 over the V sites.

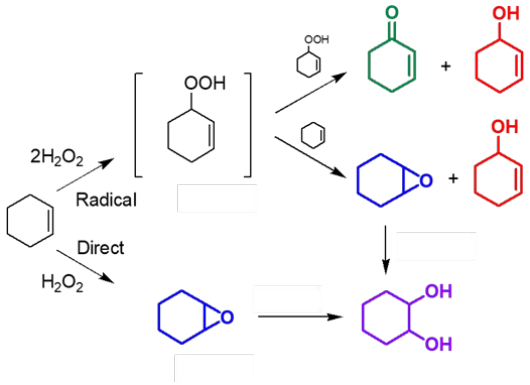

Scheme 1. Proposed reaction network for liquid-phase cyclohexene oxidation. Cyclohexenyl hydroperoxide is not detected directly. Not shown are H_2O and O_2 required to balance the reactions.

In previous reports, the initial cyclohexene TOF of a highly dispersed V-SiO_2 was 0.94 mol_{C6} mol_v^{-1} min^{-1} and cyclohexenol and cyclohexenone were dominant products, under similar conditions. [27] Therefore, MIL-47(V) shows comparable performance to a benchmark material, even though the structures of the two catalysts are quite dissimilar (e.g. isolated VO_x on silica vs. extended V-O-V chains coordinated to carboxylates).

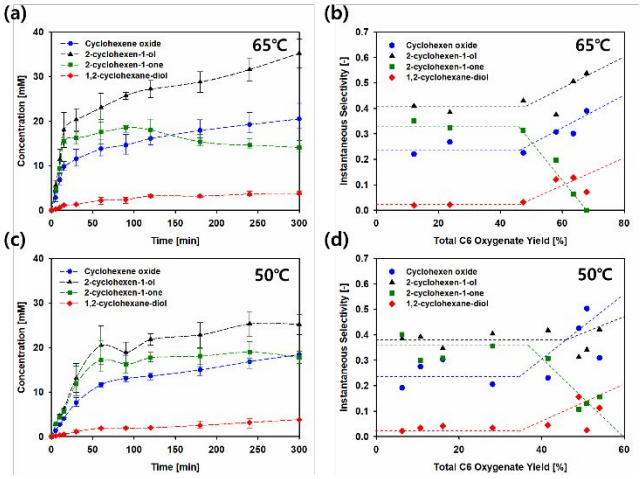

Figure 3. (a, c) Product yields vs. time and (b, d) product instantaneous selectivity vs. conversion for liquid-phase cyclohexene epoxidation with MIL-47(V) at 65 and 50 ℃. Instantaneous selectivity considers only the additional products formed between the prior time point and the current one. Lines are intended only as guides to the eye.

For the data in Figure 3(a), rates decrease by more than 10-fold after the first 15 min (~ 50 % yield of C_6 oxygenates with respect to limiting H_2O_2) to a TOF of 0.04 mol_{C6} mol_v^{-1} min^{-1}. In addition, the selectivity to cyclohexenone drops rapidly, while the selectivity to cyclohexenol rises and becomes comparable to the sum of epoxide and diol. Therefore, at later times or conversion, it appears that the primary route of C_6 oxygenate formation is through the middle cyclohexenyl hydroperoxide radical route of Scheme 1. Some of cyclohexenyl hydroperoxide species may be selectively decomposing to cyclohexenol as well. This is consistent with little to no H_2O_2 remaining in solution, and O_2 becoming the terminal oxidant.

To verify the heterogeneity of the catalytic reaction, a hot filtration experiment was performed. Leaching of active species during reaction is commonly observed for vanadium oxide-based catalysts. [14, 27-32] However, our study found no evidence for leaching of an active species. As shown in Figure 4, the reaction mixture containing MIL-47(V) was filtered at 15 min at 65 ℃ using a syringe filter, and no further product formation is detected over the next 3 h. Moreover, the ICP-OES measurements of the catalyst before and after reaction remains constant as 0.9 ± 0.1 vanadium ions per organic linker.

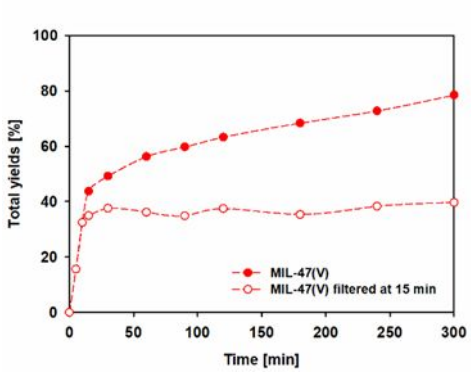

Figure 4. Leaching test of MIL-47(V) of cyclohexene epoxidation at 65 ℃.

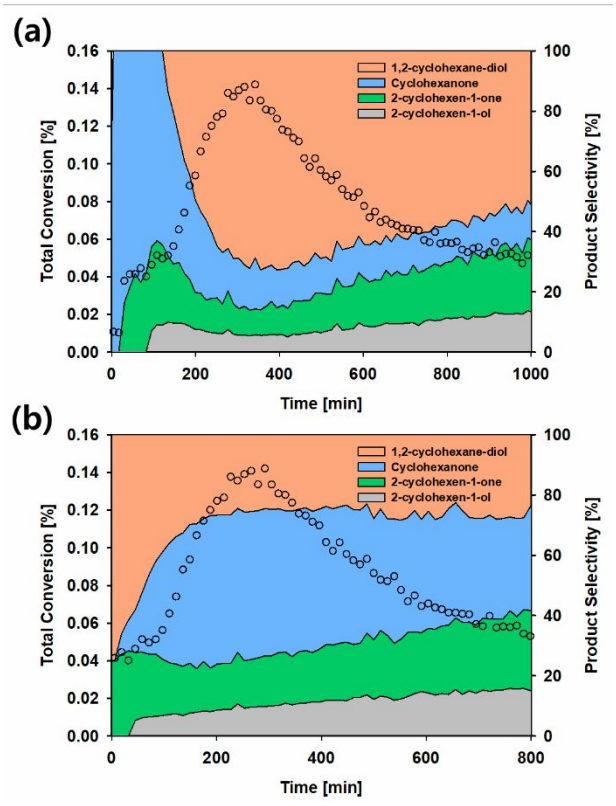

Figure 5. Time-on-stream conversion and C_6 oxygenate selectivity profile of gas-phase cyclohexene epoxidation at (a) 120 and (b) 150 ℃ over MIL-47(V). The time required for product breakthrough is likely related to the affinity of the species for the MOF pore, with ketones being adsorbed less strongly than alcohols, which are absorbed less strongly than the diol.

Gas-phase epoxidation

Gas-phase epoxidation was performed at higher temperatures (120 and 150 ℃) than the corresponding condensed-phase reaction. Figure 5(a) shows the detailed product distributions for MIL-47(V) catalyst at 120 ℃. Data at 150 ℃ are found in Figure 5(b) and shows more selectivity toward cyclohexanone. However, the C_6 oxygenate production rates at 120 ℃ are 36 % higher than at 150 ℃. This arises from increasing rates of unselective H_2O_2 decomposition in the framework at higher temperatures, which decreases the H_2O_2 concentration available for oxygenate formation. This has been observed in prior works. [7, 22, 33] At both temperatures, there is a relatively slow approach to steady reactor operation. Products take as much as 2 h time on stream (TOS) to become detectable in the reactor outlet. This is presumably due to the relatively low amounts of production and the strong affinity for some of the products (e.g. diol) to the catalyst surface in the absence of solvent. The yield of C_6 oxygenates (0.6 % with respect to limiting H_2O_2) in the steady conversion regime (> 800 min) is much lower than the yields achieved in condensed phase batch reactors, but this is expected from the much lower contact time in the flow reactor (1.1 s), and would be remedied in commercial practice by the use of additional catalyst or slower flow rates. Cyclohexenone and cyclohexenol formation rates reach a steady state in those first 3 h TOS, but it takes nearly 800 min for the total production of C_6 oxygenates to stabilize.

More significantly, the product distribution is also different in the two modes of operation. In the gas-phase flow reactor, no epoxide was observed, and at steady state (TOS > 800 min), diol is the dominant product at ~ 50% selectivity. As in the liquid phase, only the trans-diol product is observed, indicating that the diol is derived from the hydrolysis of cyclohexene epoxide. In control experiments, added epoxide and water are only partially hydrolyzed by an empty reactor, so over this catalyst, hydrolysis appears to be rapid compared to the initial epoxidation. This is specifically in contrast with previous gas-phase epoxidation over Ti/Nb-SiO_2 and Ti/Nb-NU-1000, where epoxide was observed. [22] Cyclohexenone and cyclohexenol formed with ~ 20-25 % and ~ 10-15 % selectivity at reactor steady state. Unlike in the condensed phase, gas-phase oxidation also yields 10-15 % of the saturated product cyclohexanone. The selectivity to these three products increase with time, but stay in parallel.

Cyclohexenone and cyclohexenol are formed from radical oxidation at the allylic C-H bond via an intermediate cyclohexenyl hydroperoxide. Cyclohexanone could arise either from isomerization of epoxide, dehydration of the diol, or from direct radical attack at the C=C bond. Because cyclohexenone, cyclohexenol, and cyclohexanone all increase in selectivity in parallel – and in contrast to a drop in diol (derived from epoxide) selectivity – we assume it is more likely that cyclohexanone is also formed from a radical route. We suggest that cyclohexanone is formed by hydroxyl radical attack on vinylic carbon as the temperature rises. We interpret the overall pattern of product selectivity as indicating a slow conversion of a heterolytic H_2O_2 activation site for direct epoxidation, into a site more prone to homolytic activation of H_2O_2 and subsequent radical oxidation of cyclohexene. Scheme 2 describes the proposed reaction networks toward radical and direct pathways in the gas phase.

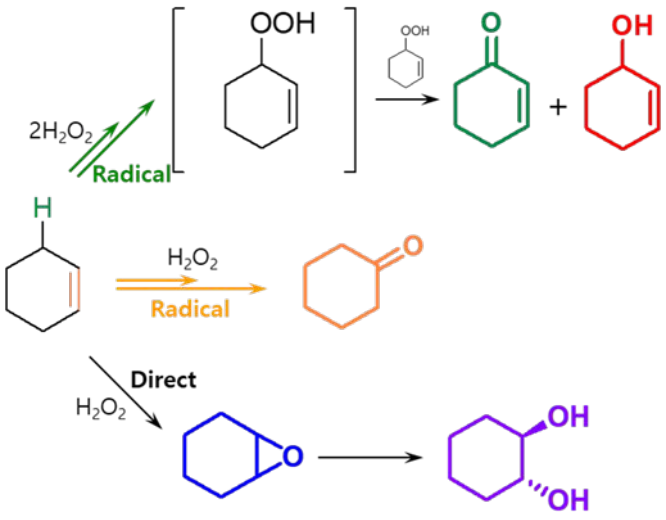

Scheme 2. Proposed reaction network for gas-phase cyclohexene oxidation. Not shown are H_2O and O_2 required to balance the reactions.

Conclusions

MIL-47(V) is an effective catalyst for the production of C_6 oxygenates from cyclohexene and H_2O_2 in both the liquid and the gas phases at temperatures between 50 and 150 ℃. In all cases, PXRD confirms framework stabilities after reaction, and there was no evidence for leaching of an active species in the liquid-phase oxidation experiment.

Most importantly, we observe significant differences in product selectivity between liquid-phase and gas-phase operations. In the case of liquid-phase epoxidation at 50 and 65 ℃ , epoxide, cyclohexenol, and cyclohexenone are primary products. While there is sufficient H_2O_2, epoxide is formed directly from cyclohexene, and radical-derived cyclohexenyl hydroperoxide species give rise to the enol and enone products in similar amounts. Relatively small amounts of the hydrolysis product (diol) are formed. In the gas-phase catalytic reaction at 120 and 150 ℃, diol (formed from epoxide) is the dominant product. The catalyst takes a long time to reach steady state conversion, then slowly changes in selectivity from one favoring direct oxidation pathways, to one that favors radical oxidation pathways. In contrast to reaction in the condensed phase, gas-phase radical products also include cyclohexanone.

Overall, these results demonstrate that a MOF with catalytically active VO_x nodes/channels can give activity in liquid phase oxidation of cyclohexene with H_2O_2 that is similar to an

oxide-supported VO_x catalyst. However, because the VO_x species are tightly incorporated into the MOF as nodes channels, these species are resistant to leaching. This work also finds that these catalysts are active in the gas phase oxidation of cyclohexene with H_2O_2 and that the frameworks remain intact even under these conditions. At the higher temperature gas-phase conditions, saturated oxygenates (cyclohexanone and diol) dominate, whereas allylic oxidation products (cyclohexenol and cyclohexenone) dominate at lower temperatures. Further studies in the gas phase will seek to understand the particular roles played by the absence of reaction solvent as well as the higher reaction temperature. This work can potentially help better understanding of alkene epoxidation in the liquid- and gas-phase over unconventional catalysts like catalytic node MOFs.

Conflicts of interest

There are no conflicts to declare.

Acknowledgements

The authors gratefully acknowledge the financial support from the Inorganometallic Catalyst Design Center, an EFRC funded by the DOE, Office of Basic Energy Sciences (DESC0012702). This work was also supported by the National Research Foundation of Korea under Grant Nos. NRF-2019R1A2C2002313.

Notes and references

1. S. Kitagawa, R. Kitaura and S.-i. Noro, *Angewandte Chemie International Edition*, 2004, **43**, 2334-2375.
2. A. J. Howarth, Y. Liu, P. Li, Z. Li, T. C. Wang, J. T. Hupp and O. K. Farha, *Nature Reviews Materials*, 2016, **1**, 15018.
3. J. L. Rowsell and O. M. Yaghi, *Microporous and Mesoporous Materials*, 2004, **73**, 3-14.
4. G. Férey, *Chemical Society Reviews*, 2008, **37**, 191-214.
5. N. Jiang, Z. Deng, S. Liu, C. Tang and G. Wang, *Korean Journal of Chemical Engineering*, 2016, **33**, 2747-2755.
6. P. Bassler, M. Weidenbach and H. Goebbel, *Chemical Engineering Transactions*, 2010, **21**, 571-576.
7. S. Kwon, N. M. Schweitzer, S. Park, P. C. Stair and R. Q. Snurr, *Journal of Catalysis*, 2015, **326**, 107-115.
8. T. Sreethawong, Y. Yamada, T. Kobayashi and S. Yoshikawa, *Journal of Molecular Catalysis A: Chemical*, 2005, **241**, 23-32.
9. C. W. Jones, *Applications of hydrogen peroxide and derivatives*, Royal Society of Chemistry, 2007.
10. R. A. Sheldon and H. Van Bekkum, *Fine chemicals through heterogeneous catalysis*, John Wiley & Sons, 2008.
11. W. Fan, P. Wu and T. Tatsumi, *Journal of Catalysis*, 2008, **256**, 62-73.
12. A. Agarwala and D. Bandyopadhyay, *Catalysis letters*, 2008, **124**, 256-261.
13. G. Langhendries, D. E. De Vos, G. V. Baron and P. A. Jacobs, *Journal of Catalysis*, 1999, **187**, 453-463.
14. K. Leus, M. Vandichel, Y.-Y. Liu, I. Muylaert, J. Musschoot, S. Pyl, H. Vrielinck, F. Callens, G. B. Marin and C. Detavernier, *Journal of Catalysis*, 2012, **285**, 196-207.
15. M. Vandichel, S. Biswas, K. Leus, J. Paier, J. Sauer, T. Verstraelen, P. Van Der Voort, M. Waroquier and V. Van Speybroeck, *ChemPlusChem*, 2014, **79**, 1183-1197.
16. J. Lee, O. K. Farha, J. Roberts, K. A. Scheidt, S. T. Nguyen and J. T. Hupp, *Chemical Society Reviews*, 2009, **38**, 1450-1459.
17. S. Ahn, N. E. Thornburg, Z. Li, T. C. Wang, L. C. Gallington, K. W. Chapman, J. M. Notestein, J. T. Hupp and O. K. Farha, *Inorganic chemistry*, 2016, **55**, 11954-11961.
18. K. Leus, I. Muylaert, M. Vandichel, G. B. Marin, M. Waroquier, V. Van Speybroeck and P. Van Der Voort, *Chemical Communications*, 2010, **46**, 5085-5087.
19. K. Barthelet, J. Marrot, D. Riou and G. Férey, *Angewandte Chemie International Edition*, 2002, **41**, 281-284.
20. P. Llewellyn, F. R. Reinoso, J. Rouqerol and N. Seaton, *Characterization of porous solids VII: proceedings of the 7th International Symposium on the Characterization of Porous Solids (COPS-VII), Aix-en-Provence, France, 26-28 May 2005*, Elsevier, 2006.
21. Y.-S. Bae, A. O. z. r. Yazaydın and R. Q. Snurr, *Langmuir*, 2010, **26**, 5475-5483.
22. S. Ahn, S. L. Nauert, K. E. Hicks, M. A. Ardagh, N. M. Schweitzer, O. K. Farha and J. M. Notestein, *ACS Catalysis*, 2020, **10**, 2817-2825.
23. N. A. Khan, J. W. Jun, J. H. Jeong and S. H. Jhung, *Chemical Communications*, 2011, **47**, 1306-1308.
24. N. Morlanés and J. M. Notestein, *Journal of Catalysis*, 2010, **275**, 191-201.
25. J. M. Fraile, J. I. Garćia, J. A. Mayoral and E. Vispe, *Applied Catalysis A: General*, 2003, **245**, 363-376.
26. J. M. Fraile, J. I. García, J. A. Mayoral and E. Vispe, *Journal of Catalysis*, 2005, **233**, 90-99.
27. N. E. Thornburg, A. B. Thompson and J. M. Notestein, *ACS Catalysis*, 2015, **5**, 5077-5088.
28. R. Neumann and M. Levin-Elad, *Applied Catalysis A: General*, 1995, **122**, 85-97.
29. H. Salavati and A. Teimouri, *Int. J. Electrochem. Sci*, 2017, **12**, 7829-7843.
30. J. S. Reddy, P. Liu and A. Sayari, *Applied Catalysis A: General*, 1996, **148**, 7-21.
31. K. Kang and W. Ahn, *Journal of Molecular Catalysis A: Chemical*, 2000, **159**, 403-410.
32. C. Tiozzo, C. Palumbo, R. Psaro, C. Bisio, F. Carniato, A. Gervasini, P. Carniti and M. Guidotti, *Inorganica Chimica Acta*, 2015, **431**, 190-196.
33. C. Satterfield and T. Stein, *Industrial & Engineering Chemistry*, 1957, **49**, 1173-1180.

Table of Contents

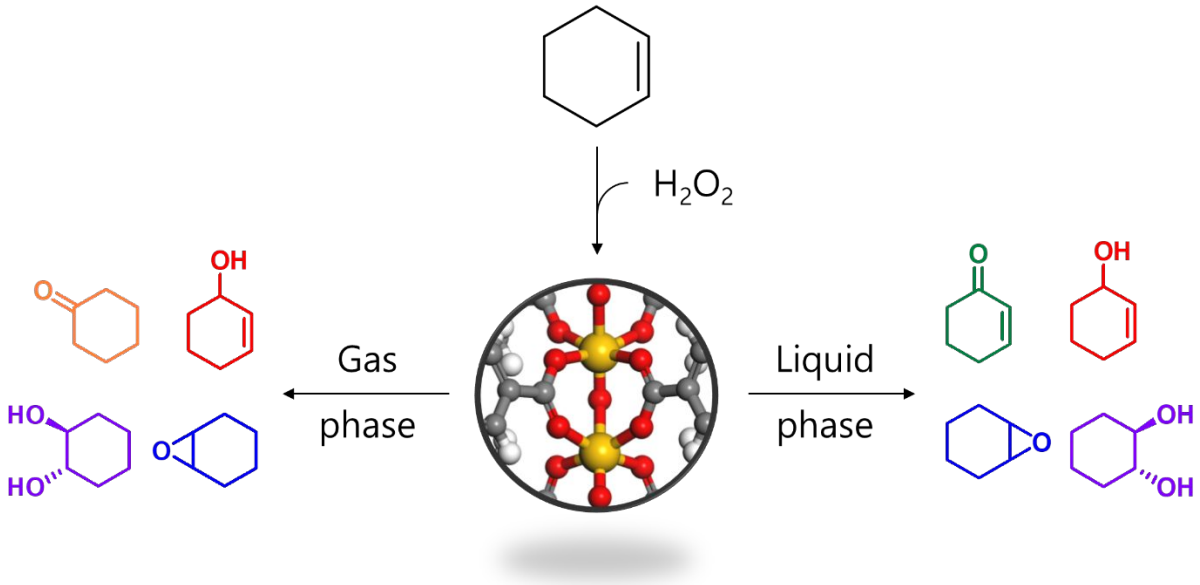

A V-containing metal-organic framework exhibits significant different catalytic mechanisms between liquid-phase and gas-phase cyclohexene oxidations.